[American Journal of Science, Vol. 306, September, 2006, P. 553–574, DOI 10.2475/07.2006.03]

CRYSTALLIZATION KINETICS IN BINARY SOLID SOLUTION–AQUEOUS SOLUTION SYSTEMS

ALEXANDER G. SHTUKENBERG*[,†], YURII O. PUNIN*, and PAVEL AZIMOV**

ABSTRACT. Phenomenological description of crystallization kinetics in a binary system "aqueous solution–solid solution" is given. This approach involves consideration of the true equilibrium and possible quasi-equilibrium states. It gives description of the crystallization kinetics close to equilibrium and features of the growth process occurring at high driving forces and growth rates. Special attention is paid to interactions between an aqueous solution and a seed crystal placed into this solution. In particular, this includes analysis of pure chemical interactions as well as effect of misfit strain. The theory developed predicts the growth/dissolution rate of a mixed crystal based on the knowledge of phase diagram and growth kinetics of the end members of the series. The key point of the paper is discussion of supersaturation concept in such aqueous solution–solid solution systems.

GLOSSARY OF SYMBOLS

a	activity of ions in aqueous solution
b	lattice constant
c	ion concentration in an aqueous solution
f	activity coefficient of components in solid solution
k	kinetic coefficient
k^+, k^-	kinetic coefficients for direct and reverse reactions, respectively
w	molar volume
x	molar fraction of components in solid solution
y	activity fraction in the salt part of aqueous solution $y = a_i/(a_B + a_C)$
D	distribution coefficient
E	Young modulus
J^+, J^-, J	direct, reverse and total fluxes of components, respectively
K	solubility product
R	universal gas constant
T	absolute temperature
U	stress energy
V	linear growth rate
γ	activity coefficient of components in aqueous solution
β, δ, ξ	different supersaturation functions
ε_j	components of the strain tensor
μ	chemical potential
$\Delta\mu$	difference in chemical potentials
ν	Poisson ratio
σ_j	components of the stress tensor
$\Sigma\Pi$	total activity product (total solubility product in the case of equilibrium)

Subscripts

i = A, B, C	ions in aqueous or solid solution
iA = BA, CA	components of solid solution

---

*St. Petersburg State University, Universitetskaya emb., 7/9, 199034, St. Petersburg, Russia; sasha@as3607.spb.edu

**Institute of Precambrian Geology and Geochronology, Makarov emb., 2, 199034, St. Petersburg, Russia

eq	equilibrium
s	substrate
st	stoichiometric saturation
U	elastic stress is taken into account
∞	approximation of infinitely high growth rate

Superscripts

aq	aqueous solution
ss	solid solution
0	standard state
$n+$, $n-$	charges of ions in aqueous solution

INTRODUCTION

The phenomenological theory of crystallization of simple salts from aqueous solutions is developed well enough to predict the crystal growth/dissolution rate provided the data on solubility, solution composition and a few kinetic constants are known. However, a significant number of minerals and industrially important synthetic compounds are solid solutions, whose formation from aqueous solution is not yet understood in full detail. Crystallization in such "solid solution – aqueous solution" systems (SS-AS systems) was a subject of experimental and theoretical studies performed during the last few decades. In particular, a success was achieved in understanding phase equilibria, and in simulation of Lippmann SS-AS phase diagrams (Lippmann, 1980; Glynn and Reardon, 1990; Glynn and others, 1990; Glynn, 2000) and of their modifications (Treivus, 2000; Azimov and Shtukenberg, 2000; Shtukenberg and Azimov, 2001).

Experimental data on crystallization kinetics of mixed crystals were reported in a few papers only (Zhmurova and Khaimov-Mal'kov, 1970a, 1970b; Tsuchiyama and others, 1981; Mullin and Kitamura, 1985; Kasatkin and others, 1995; Soloviev and others, 1997; Wasylenki and others, 2005). Several authors considered quasi-equilibria and replacement processes between aqueous and solid solutions (Glikin, 1995, 1996; Kryuchkova and others, 2002; Putnis, 2002; Glikin and others, 2003; Voloshin and others, 2003a, 2003b; Putnis and Mezger, 2004;) and the effect of elastic stress during crystal growth (Bolkhovityanov, 1982; Moshkin and others, 2000). Finally some atomic force microscopic (AFM) studies of crystal growth in SS-AS systems were performed recently (Davis and others, 2000; Astilleros and others, 2003b; Sánchez-Pastor, 2005; Shtukenberg and others, 2005).

A. A. Chernov (Voronkov and Chernov, 1967; Chernov, 1970, 1984) has developed a statistical theory of isomorphous impurities incorporation, which was applicable for minor concentrations but failed to deal with higher concentrations of dopants. Van Erk (1982) formulated the theory of growth, which was based on the thermodynamics of irreversible processes but contained some unclear points and ignored the role of substrate. In addition, certain works on thermodynamics of nucleation and growth kinetics in binary "solid solution–liquid solution" systems can be mentioned (Kamenetskaya, 1968; Temkin, 1980, 1981), whose results may also be applied to SS-AS systems.

The key point of the growth in SS-AS systems is determination of supersaturation or, more precisely, of the driving force of crystallization. A pure thermodynamic approach gives no way to construct the single variable as the chemical potentials of components in both solid and aqueous solutions are mutually independent. For example, this approach ignores situation, when the difference in chemical potentials between solid and aqueous solutions is positive for one component and negative for the second one. This situation is, however, typical for many natural systems and should be clarified.

The second problem is that any driving force expression must include the compositions of both aqueous and solid solutions. However the latter is not known *a priori* and thermodynamic consideration provides only a hypothetical way to predict it.

The last, but not the least problem concerns the misfit strain arising at the interface between substrate and a new deposited layer of different composition. This has a strong effect on the thermodynamics and kinetics of crystal growth.

In this study we intend to consider theoretically the main features of solid solution formation from aqueous solutions starting from the equilibrium and quasi-equilibrium in SS-AS systems, looking at crystallization kinetics under the simplest growth conditions and under more complicated ones.

DESCRIPTION OF THE SYSTEM

We consider a simple SS-AS system (B,C)A – H_2O, where the cations B^{n+} and C^{n+} and the anion A^{n-} are present in the aqueous solution and form a continuous series of solid solutions. The aqueous solution can contain some other species, which do not incorporate into the crystal. They can indirectly affect SS-AS partitioning through speciation, complexation and effects on the ionic strength. These influences, however, can be taken into account by appropriated choice of the activity coefficients and are not considered here. We ignore the nucleation and mass transport processes like diffusion and consider only the kinetics of species attachment/detachment occurring at the edges of steps spreading along the flat crystal surface with the surface reaction as the rate-limiting factor. After some simple rearrangements the results can be also applied to the normal growth rates. If other is not specified, we also assume that the crystal is very small compared with the amount of aqueous solution, so that the aqueous solution does not change its composition during the growth/dissolution processes.

The crystal growth is a transition from one phase (aqueous solution denoted below by the superscript *aq*) to another one (solid solution denoted by the superscript *ss*), so it can be considered as a *heterogeneous* chemical reaction. The net reaction should be written as follows:

$$x_{BA}B^{n+} + x_{CA}C^{n+} + A^{n-} = B_{x_{BA}}C_{x_{CA}}A, \tag{1}$$

where the right side of the equation relates to the solid solution and the left one–to the aqueous solution; x_{CA} and $x_{BA} = 1 - x_{CA}$ are the mole fractions of the components BA and CA in the solid solution, respectively. Note that due to the mass balance requirement the fractional stoichiometric coefficients x_{BA} and x_{CA} appear in the left side of the equation (aqueous solution side). From the point of view of thermodynamic equilibrium this reaction is not valid. Indeed the equilibrium conditions for this reaction (the chemical affinity is equal to zero) does not necessarily result in the equality of chemical potentials of each component in both phases. Thus the stoichiometric coefficients of any heterogeneous reaction should be restricted by the values of ±1 (Prigogine and Defay, 1954). It is necessary to consider two independent reactions coupled only by the mass balance condition $x_{BA} + x_{CA} = 1$:

$$B^{aq} + A^{aq} = BA^{ss} \tag{2}$$

$$C^{aq} + A^{aq} = CA^{ss} \tag{3}$$

Therefore, equilibrium and the driving forces leading to it are defined by *two* quasi-independent chemical reactions.

EQUILIBRIUM

The chemical potential of each component in the aqueous solution is

$$\mu_i^{aq} = \mu_i^{0aq} + RT \ln a_i = \mu_i^{0aq} + RT \ln c_i\gamma_i \quad i = \text{A, B, C} \tag{4}$$

where a_i, c_i and γ_i is the *i*-th ion activity, concentration and activity coefficient respectively, R is the gas constant, T is the absolute temperature. The superscript ^{0} refers to the standard state. For the solid solution the corresponding equations have the form

$$\mu_{iA}^{ss} = \mu_{iA}^{0ss} + RT \ln f_{iA} x_{iA} \quad i = \mathrm{B, C} \tag{5}$$

Here $x_{i\mathrm{A}}$ and $f_{i\mathrm{A}}$ are the molar fraction and the activity coefficient of *i*-th components in the solid solution.

In equilibrium $\mu_{iA}^{ss} = \mu_{iA}^{aq} = \mu_i^{aq} + \mu_A^{aq}$. It gives the conditions one needs to calculate the equilibrium phase diagram

$$\Delta\mu_{\mathrm{BA}}^0 = \mu_{\mathrm{BA}}^{0ss} - \mu_{\mathrm{B}}^{0aq} - \mu_{\mathrm{A}}^{0aq} = RT \ln\left(\frac{a_{\mathrm{B}eq} a_{\mathrm{A}eq}}{f_{\mathrm{BA}} x_{\mathrm{BA}}}\right) \tag{6}$$

$$\Delta\mu_{\mathrm{CA}}^0 = \mu_{\mathrm{CA}}^{0ss} - \mu_{\mathrm{C}}^{0aq} - \mu_{\mathrm{A}}^{0aq} = RT \ln\left(\frac{a_{\mathrm{C}eq} a_{\mathrm{A}eq}}{f_{\mathrm{CA}} x_{\mathrm{CA}}}\right) \tag{7}$$

The subscript *eq* denotes the equilibrium. The expressions (6) and (7) are valid for any fraction $x_{i\mathrm{A}}$, in particular for $x_{\mathrm{BA}} = 1$ and $x_{\mathrm{CA}} = 1$. Substitution of the variables yields

$$\Delta\mu_{\mathrm{BA}}^0 = RT \ln K_{\mathrm{BA}} \tag{8}$$

$$\Delta\mu_{\mathrm{CA}}^0 = RT \ln K_{\mathrm{CA}} \tag{9}$$

where K_{BA} and K_{CA} are the solubility products of the end members of the series. Finally we have the general expressions for the computation of the phase diagram

$$a_{\mathrm{B}eq} a_{\mathrm{A}eq} = f_{\mathrm{BA}} K_{\mathrm{BA}} x_{\mathrm{BA}} \tag{10}$$

$$a_{\mathrm{C}eq} a_{\mathrm{A}eq} = f_{\mathrm{CA}} K_{\mathrm{CA}} x_{\mathrm{CA}} \tag{11}$$

At this point it is useful to introduce the total ion activity product variable IAP = $a_{\mathrm{A}}(a_{\mathrm{B}} + a_{\mathrm{C}})$, which characterizes the solution and below is always denoted as $\Sigma\Pi$. In a similar manner for the equilibrium we introduce the total solubility product variable $\Sigma\Pi_{eq} = a_{\mathrm{A}eq}(a_{\mathrm{B}eq} + a_{\mathrm{C}eq})$ (Lippmann, 1980), which directly leads us to the *solidus* equation of the system

$$\Sigma\Pi_{eq} = f_{\mathrm{BA}} K_{\mathrm{BA}} x_{\mathrm{BA}} + f_{\mathrm{CA}} K_{\mathrm{CA}} x_{\mathrm{CA}}. \tag{12}$$

In order to derive the solutus equation we introduce the activity fraction of *i*-th component in the salt part of aqueous solution is $y_i = a_i/(a_{\mathrm{B}} + a_{\mathrm{C}})$ $(i = \mathrm{B, C})$. Combining equations (10), (11) and (12) with definition of y_i gives

$$\frac{y_{\mathrm{B}}}{f_{\mathrm{BA}} K_{\mathrm{BA}}} = \frac{x_{\mathrm{BA}}}{\Sigma\Pi_{eq}} \tag{13}$$

$$\frac{y_{\mathrm{C}}}{f_{\mathrm{CA}} K_{\mathrm{CA}}} = \frac{x_{\mathrm{CA}}}{\Sigma\Pi_{eq}} \tag{14}$$

and thereby provides an expression for the *solutus* of the system

$$\Sigma\Pi_{eq} = \frac{1}{\dfrac{y_{\mathrm{B}}}{f_{\mathrm{BA}} K_{\mathrm{BA}}} + \dfrac{y_{\mathrm{C}}}{f_{\mathrm{CA}} K_{\mathrm{CA}}}} \tag{15}$$

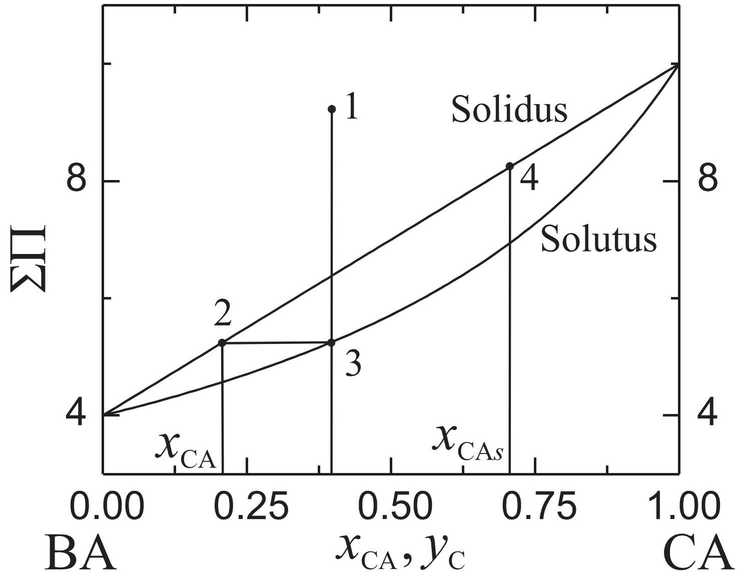

Fig. 1. Lippmann diagram for a hypothetical ideal aqueous solution - solid solution system. The solubility products of the end members are $K_{BA} = 4$, $K_{CA} = 10$, the equilibrium distribution coefficent $D_{eq} = K_{CA}/K_{BA} = 0.4$.

The typical phase diagram of a system with continuous series of solid solutions is shown in figure 1. The way we used above to describe the phase equilibria in a SS-AS system has first been proposed by Lippmann (1980) and further developed in a series of works (Glynn and Reardon, 1990; Glynn and others, 1990; Glynn, 2000). Some modifications suitable for highly soluble salts were added by us (Azimov and Shtukenberg, 2000; Shtukenberg and Azimov, 2001).

To complete the set of equations, which characterizes the true equilibrium in a SS-AS system the equilibrium distribution coefficient should be introduced. This variable is usually defined as (Henderson and Kracek, 1927)

$$D^{\#}_{eq} = \frac{x_{BA}}{x_{CA}} \cdot \frac{c_C}{c_B} = \frac{x_{BA}}{x_{CA}} \cdot \frac{a_C \gamma_B}{a_B \gamma_C} = \frac{x_{BA}}{x_{CA}} \cdot \frac{y_C}{y_B} \cdot \frac{\gamma_B}{\gamma_C} \qquad (16)$$

The superscript $^{\#}$ is added only to distinguish this definition of distribution coefficient from that given below. On the other hand, it can be deduced theoretically from the solubility products of the end members of the series (Ratner, 1933; Azimov and Shtukenberg, 2000). In our notations this result can be obtained directly from the equations (13) and (14):

$$D^{\#}_{eq} = \frac{K_{CA} f_{CA} \gamma_B}{K_{BA} f_{BA} \gamma_C} \qquad (17)$$

Through the manuscript we are dealing with activity fractions $y_i = a_i/(a_B + a_C)$ instead of concentration fractions $c_i/(c_B + c_C)$. Therefore, to avoid confusion and for the sake of simplicity we introduce the equilibrium distribution coefficient in some other form

$$D_{eq} = \frac{x_{BA}}{x_{CA}} \cdot \frac{a_C}{a_B} = \frac{K_{CA}}{K_{BA}} \cdot \frac{f_{CA}}{f_{BA}} \qquad (18)$$

This correction does not change the meaning and general behavior of this variable and the "standard" distribution coefficient can be always found if the activity coefficients are known.

Below we use the Lippmann phase diagrams as a starting point for the description of crystallization kinetics.

QUASI-EQUILIBRIA

In the previous section the true thermodynamic equilibrium between solid solution and aqueous solution has been considered. Here we are going to treat the quasi-equilibria that is the states, when the thermodynamic equilibrium is not achieved, but the driving force for the ionic fluxes of one or both components between aqueous solution and solid solution can be negligible. To do it we can consider the solid solution as a mixture of two components (BA and CA) and find the conditions for the equilibrium of each component separately with respect to a series of aqueous solutions in accordance with the reactions (2) and (3), respectively. In this way we find the states, when the chemical potential difference between solid and aqueous solutions $\Delta G_{i\mathrm{A}} = \mu_{i\mathrm{A}}^{ss} - \mu_i^{eq} - \mu_{\mathrm{A}}^{aq}$ for one of the components iA is equal to zero, but for the second one it can take on different values (positive, negative or zero). In other words, we fix the composition of solid solution to be $x_{\mathrm{BA}s} = 1 - x_{\mathrm{CA}s}$ and explore behavior of the partial solubility product $\Sigma\Pi$ as a function of either y_{B} or y_{C}. Such a condition can be directly deduced from the equations (13) and (14) as follows

$$\Sigma\Pi_{\mathrm{B}eq} \equiv \Sigma\Pi_{eq}(y_{\mathrm{B}}) = \frac{K_{\mathrm{BA}} f_{\mathrm{BA}s} x_{\mathrm{BA}s}}{y_{\mathrm{B}}} \tag{19}$$

$$\Sigma\Pi_{\mathrm{C}eq} \equiv \Sigma\Pi_{eq}(y_{\mathrm{C}}) = \frac{K_{\mathrm{CA}} f_{\mathrm{CA}s} x_{\mathrm{CA}s}}{y_{\mathrm{C}}} \tag{20}$$

These functions take on values of $K_{i\mathrm{A}} f_{i\mathrm{A}s} x_{i\mathrm{A}s} \leq K_{i\mathrm{A}}$ if $y_i = 1$, tend to infinity for $y_i \to 0$ and correspond to the hyperbolas in the Lippmann diagram (fig. 2). Each hyperbola describes equilibrium of given solid solution with aqueous solution relative to one individual component. The point of their intersection (point O in fig. 2) corresponds to the true equilibrium $\Sigma\Pi_{\mathrm{B}eq} = \Sigma\Pi_{\mathrm{C}eq} = \Sigma\Pi_{eq}$ (a solid solution is in equilibrium with the one and the same aqueous solution with respect to both components) and thus belongs to the *solutus.* Above (below) the corresponding line the chemical potential of component $i\mathrm{A} = \mathrm{BA}, \mathrm{CA}$ in aqueous solution of composition y_i is higher (lower) than the chemical potential of this component in a given solid solution $x_{\mathrm{CA}s}$. Respectively, these two hyperbolas divide the phase space into the four regions, marked in figure 2 by roman numbers. The aqueous solutions in the region I are supersaturated with respect to both the components BA and CA. On the contrary, the solutions in the region III are undersaturated with respect to both the components. The other two regions represent the aqueous solutions supersaturated with respect to one component and undersaturated with respect to the other one of the solid solution in question. Thus these lines describe equilibrium of solid and aqueous solutions to each component separately and therefore can represent the true equilibrium only in the point O. As it will be shown below, these lines turn out to be very useful for the description of interaction between aqueous and solid solutions.

Another useful quasi-equilibrium state can be deduced considering the crystal dissolution. This process involves detachment of the cations B^{n+} and C^{n+} in the same proportion in which they are present in the solid solution. Thus the crystal dissolves congruently (as a whole), and this process can be described by the net reaction (1). In accordance with the law of mass action the dissolution stops when the solution acquires certain concentration of components and the system achieves the so-called *stoichiomet-*

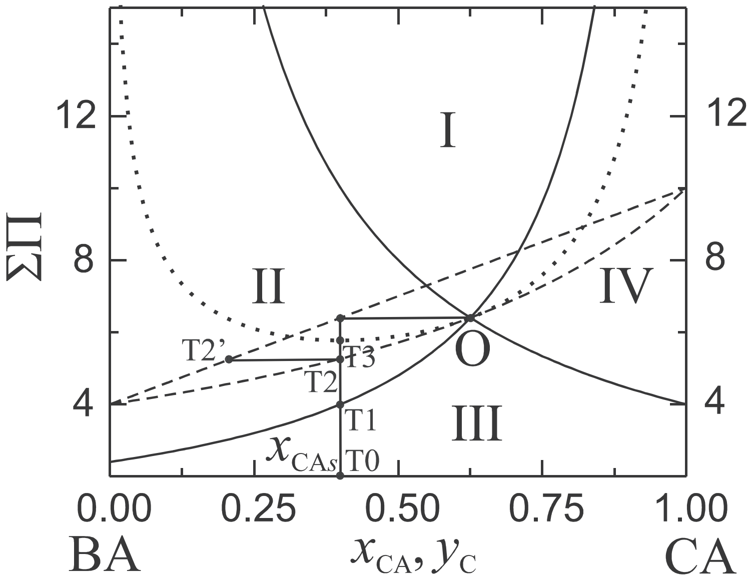

Fig. 2. Quasi-equilibria for the SS-AS system shown in fig. 1 (the equilibrium phase diagram is shown by dashed lines). Solid lines show equilibrium of the solid solution $x_{CAs} = 0.4$ with respect to the whole series of aqueous solutions. Regions separated by solid lines and marked by the roman numbers denote: I (gray background) supersaturation with respect to both the components BA and CA; II supersaturation with respect to CA and undersaturation with respect to BA; III (gray background) undersaturation with respect to BA and CA; IV supersaturation with respect to BA and undersaturation with respect to CA. The dotted line is stoichiometric saturation state for the same solid solution x_{Cs}.

ric saturation state defined by Thorstenson and Plummer (1977). Later development (Glynn and others, 1990; Glynn and Reardon, 1990, 1992; Glynn, 2000) transformed this concept to a powerful tool for studying the SS-AS phase diagrams. In this case the solubility product K_{st} can be found from equilibrium conditions for the net reaction (1) considering the values of x_i (i = B, C) as the stoichiometric coefficients

$$K_{st} = a_{Beq}^{x_{BA}} a_{Ceq}^{x_{CA}} a_{Aeq} = (K_{BA} f_{BA} x_{BA})^{x_{BA}} (K_{CA} f_{CA} x_{CA})^{x_{CA}} \qquad (21)$$

In contrast to the thermodynamic equilibrium, when each solid solution x_{CA} corresponds to a single aqueous solution, the stoichiometric saturation of solid solution x_{CA} is achieved for a series of aqueous solutions y_C, which are characterized by the total solubility products

$$\Sigma\Pi_{st} = \frac{K_{st}}{y_B^{x_{BA}} y_C^{x_{CA}}} = (\Sigma\Pi_{Beq})^{x_{BA}} (\Sigma\Pi_{Ceq})^{x_{CA}} \qquad (22)$$

The stoichiometric saturation curve (dotted line in fig. 2) has a minimum at $y_C = x_{CAs}$ and is tangent to the *solutus* curve at the point O related to the true equilibrium between the crystal x_{CAs} and the aqueous solution.

CRYSTAL GROWTH: THERMODYNAMIC APPROACH

The solid solution–aqueous solution interactions are not restricted to the true equilibrium and quasi-equilibria and various processes such as crystal growth, dissolution and metasomatic replacement take place. We are going to consider such processes beginning with the simplest case of "pure" crystal growth, when no reaction between the seed crystal and the solution occurs and the system is assumed to be not far from the equilibrium.

Let us consider the supersaturated solution (point 1 in fig. 1), which is characterized by the total solubility product $\Sigma\Pi$ and has the composition of y_C. Crystallization from the solution is driven by the difference in chemical potential of the liquid and the crystal

$$\Delta\mu_{BA} = \mu_B^{aq} + \mu_A^{aq} - \mu_{BA}^{ss} = RT\ln\left(\frac{a_B a_A}{f_{BA}x_{BA}}\right) - \Delta\mu_{BA}^0 = RT\ln\left(\frac{a_B a_A}{f_{BA}x_{BA}K_{BA}}\right) \quad (23)$$

$$\Delta\mu_{CA} = \mu_C^{aq} + \mu_A^{aq} - \mu_{CA}^{ss} = RT\ln\left(\frac{a_C a_A}{f_{CA}x_{CA}}\right) - \Delta\mu_{CA}^0 = RT\ln\left(\frac{a_C a_A}{f_{CA}x_{CA}K_{CA}}\right) \quad (24)$$

These equations have the same structure as (6) and (7) but now the values of $\Delta\mu_{iA}$ are not restricted to be equal to zero as it was for the equilibrium. It follows from (23) and (24) that deviation from the equilibrium depends on crystal composition as well as on the aqueous solution composition. But the composition of growing crystal x_{CA} is unknown *a priori*. To find it for the continuous series of solid solutions, which crystallize from the simple system without metastable/intermediate phases, one can assume that the crystallization provides the maximum possible decrease in the system molar free energy $\Delta G = x_{BA}\Delta\mu_{BA} + x_{CA}\Delta\mu_{CA}$, that is the condition $\partial\Delta G/\partial x_{BA} = 0$ holds (Sally, 1963; Ghiorso, 1994; Astilleros and others, 2003a). Unfortunately, although reasonable, this assumption does not have sufficient theoretical background and can be considered only as a plausible hypothesis. Like any other partial variables the chemical potentials of components can be represented as

$$\Delta\mu_{BA} = \Delta G + (1 - x_{BA})\frac{\partial\Delta G}{\partial x_{BA}} \quad (25)$$

$$\Delta\mu_{CA} = \Delta G - x_{BA}\frac{\partial\Delta G}{\partial x_{BA}} \quad (26)$$

For the case under consideration $\partial\Delta G/\partial x_{BA} = 0$ and these conditions are fulfilled only if $\Delta\mu_{BA} = \Delta\mu_{CA}$. The same result can be obtained directly by differentiating expression for the free energy ΔG and application of the Gibbs-Duhem equation (Prigogine and Defay, 1954). Evaluation of the second derivative and application of the Gibbs stability conditions shows that the extremum point found corresponds to a maximum. After substituting (25) and (26) into the equations (23) to (24), the comparison with the expressions (10), (11) and (17) shows that the crystallization from each solution of the composition y_C with any $\Sigma\Pi$ value should form the solid solution of composition x_{CA}; in other words, the distribution coefficient should always be constant and equal to the equilibrium value $D = D_{eq}$. Thus, crystallization from solution 1 gives the crystal of composition 2, which should be in equilibrium with the solution 3 (fig. 1). This allows us to use the difference in chemical potential between solutions 1 and 3 as the value of solution supersaturation, or as the driving force for crystallization. From the equations (10), (11), (23) and (24) we get

$$\Delta\mu_{BA} = RT\ln\left(\frac{a_B a_A}{a_{Beq}a_{Aeq}}\right) = RT\ln\left(\frac{y_B\Sigma\Pi}{y_{Beq}\Sigma\Pi_{eq}}\right) \quad (27)$$

$$\Delta\mu_{CA} = RT\ln\left(\frac{a_C a_A}{a_{Ceq}a_{Aeq}}\right) = RT\ln\left(\frac{y_C\Sigma\Pi}{y_{Ceq}\Sigma\Pi_{eq}}\right) \quad (28)$$

Since for $\Delta\mu_{BA} = \Delta\mu_{CA}$ the solution has a constant composition $y_i = y_{ieq}$, we can define the supersaturation function ξ as

$$\frac{\Delta\mu_{BA}}{RT} = \frac{\Delta\mu_{CA}}{RT} = \xi = \ln\left(\frac{\Sigma\Pi}{\Sigma\Pi_{eq}}\right) \approx \frac{\Sigma\Pi}{\Sigma\Pi_{eq}} - 1, \tag{29}$$

where the latter approximate equality follows from the condition of proximity to equilibrium. A similar expression was deduced by Van Erk (1982). This means that deviation of the aqueous solution from the equilibrium with solid solution is the same with respect to both the components. The growth rate can be expressed in terms of standard supersaturation $V = k(x_{iA})\xi$, where $k(x_{iA})$ is the composition dependent kinetic coefficient [see equation (41) below]. Despite the simplicity this consideration is usually sufficient for the description of experimental data (Kasatkin and others, 1995).

We would like to emphasize that this simplest case is characterized by only one value of supersaturation/undersaturation ξ, which is a thermodynamic variable describing deviation of the *aqueous solution* from the strict thermodynamic equilibrium.

CRYSTAL GROWTH: KINETIC APPROACH

The thermodynamic consideration is restricted to the crystal growth not far from equilibrium, since only near to equilibrium the proportionality between flux and driving force has been postulated and verified. Far from equilibrium chemical thermodynamics provides no tool for the crystallization description. In such cases the principles of chemical kinetics seem to be more appropriate (Lasaga, 1981). Below we will consider independent attachment/detachment of cations in accordance with the reactions (2) to (3) and, for the sake of simplicity, will ignore additional effects related to the association of ions, formation of intermediate compounds, contribution of other species *et cetera*.

The total flux of the component *i*A (i = B, C) into the crystal is a balance of the direct J^+_{iA} and reverse J^-_{iA} fluxes

$$J_{BA} = J^+_{BA} - J^-_{BA} = k^+_{BA}a_Ba_A - k^-_{BA}f_{BA}x_{BA} \tag{30}$$

$$J_{CA} = J^+_{CA} - J^-_{CA} = k^+_{CA}a_Ca_A - k^-_{CA}f_{CA}x_{CA} \tag{31}$$

where k^+_{iA} and k^-_{iA} are the kinetic coefficients of the direct and reverse reaction, respectively. We suppose that k^+_{iA} *and* k^-_{iA} are independent of liquid and solid phase composition. In a first approximation it is a plausible assumption, which follows from the chemical kinetics. Some additional effects on the kinetic coefficients are automatically taken into account by activity coefficients. Other influences are not considered in this model, but they can be easily incorporated into the model if the physical basis for such influences will be known. In equilibrium $J_{iA} = 0$, therefore

$$a_{Beq}a_{Aeq} = \frac{k^-_{BA}}{k^+_{BA}}f_{BA}x_{BA} \tag{32}$$

$$a_{Ceq}a_{Aeq} = \frac{k^-_{CA}}{k^+_{CA}}f_{CA}x_{CA} \tag{33}$$

From the equations (10) and (11) one can directly obtain

$$k^-_{BA} = k^+_{BA}K_{BA} \tag{34}$$

$$k^-_{CA} = k^+_{CA}K_{CA} \tag{35}$$

and find the kinetic expression for the equilibrium distribution coefficient

$$D_{eq} = \frac{k^+_{BA}}{k^-_{BA}} \cdot \frac{k^-_{CA}}{k^+_{CA}} \cdot \frac{f_{CA}}{f_{BA}} \tag{36}$$

Substitution of the equations (34) and (35) into (30) and (31) gives

$$J_{BA} = k^+_{BA}(a_B a_A - K_{BA} f_{BA} x_{BA}) = k^+_{BA}(y_B \Sigma\Pi - K_{BA} f_{BA} x_{BA}) \tag{37}$$

$$J_{CA} = k^+_{CA}(a_C a_A - K_{CA} f_{CA} x_{CA}) = k^+_{CA}(y_C \Sigma\Pi - K_{CA} f_{CA} x_{CA}) \tag{38}$$

As the steady state is reached, these two equations should be completed by the stationary condition

$$\frac{J_{BA}}{J_{CA}} = \frac{x_{BA}}{x_{CA}} \tag{39}$$

Assuming the kinetic coefficients are known (for example, from the kinetic data on the end members BA and CA) these three equations have three variables (J_{BA}, J_{CA}, and $x_{CA} = 1 - x_{BA}$) and can be solved. For ideal solid solutions ($f_{BA} = f_{CA} = 1$) the substitution of equations (37) and (38) into (39) gives a cumbersome quadratic equation with respect to x_{CA}. Its analytical solution describes the effect of solubility product $\Sigma\Pi$ and solution composition y_C on the distribution coefficient D. For non-ideal solid solutions the set of equations can be solved numerically.

Given the values of fluxes J_{iA} the linear growth rate is easily obtained as

$$V = w_{BA} J_{BA} + w_{CA} J_{CA} \approx w(J_{BA} + J_{CA}) \tag{40}$$

where w_B and w_C denote the molar volumes of the components ($w \equiv w_{BA} \approx w_{CA}$).

The results of a model calculation are shown in figures 3 and 4. It can be seen that the zero growth rate (equilibrium) leads to the equilibrium value of distribution coefficient $D = D_{eq}$. Respectively, in the vicinity of equilibrium ($D \approx D_{eq}$, $y_i \approx y_{ieq}$) the growth rate can be found from equations (27)–(29), (37), (38), (40) and expressed in the simple form

$$V = (k^+_{BA} K_{BA} f_{BA} x_{BA} + k^+_{CA} K_{CA} f_{CA} x_{CA}) w\xi \tag{41}$$

As the growth rate increases the distribution coefficient approaches the limiting constant value of $D_\infty = k^+_{BA}/k^+_{CA}$ (at $V \to \infty$). This follows from the fact that the reverse fluxes become negligible compared with the direct ones as the growth rate rises significantly. The same result was also obtained by Van Erk (1982).

In all the calculations the growth rate (the velocity of steps) was assumed to be proportional to the difference in activity products (that is to the supersaturation, see fig. 4). This assumption was based on the theory developed by Chernov (1984), and on the experimental data available for different compounds (Chernov and Malkin, 1988; Ristic and others, 1997). However, for certain reasons (for example, action of impurities) the $V(\xi)$ function can assume much more complicated character (Chernov and others, 1987), in which case a revision of the model would be required.

In contrast to the thermodynamic approach the kinetic one does not use the assumption of $\Delta\mu_{BA} = \Delta\mu_{CA}$. The solution follows from the set of equations (37) to (39), and evaluates the steady state with $\Delta\mu_{BA} \neq \Delta\mu_{CA}$ and variable distribution coefficient D and the crystal composition. The value of supersaturation ξ can be written for this case as well, but now it is only a formal value, which does not reflect the true deviation from the thermodynamic equilibrium and it is not sufficient to predict the

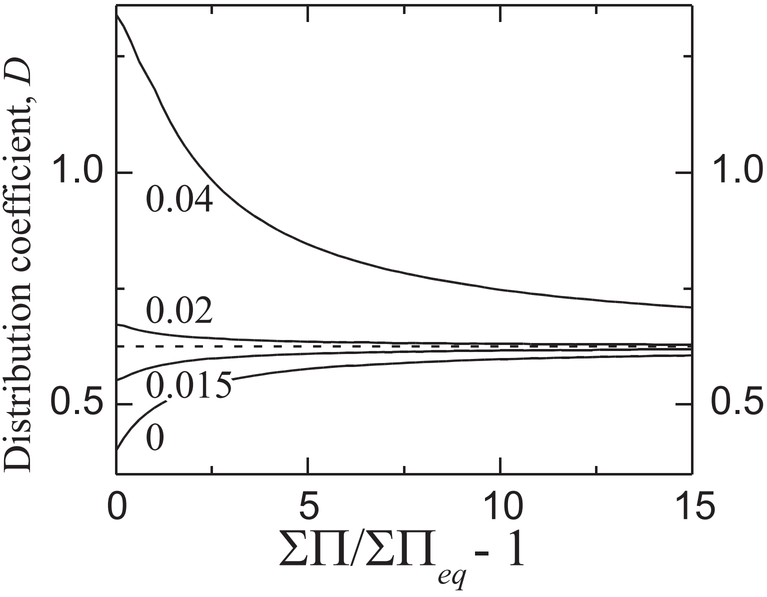

Fig. 3. Distribution coefficient D as a function of supersaturation $\Sigma\Pi/\Sigma\Pi_{eq} - 1$ for the SS-AS system shown in fig. 1. The value of lattice misfit $(b_{BA} - b_{CA})/b_s$ is written at the lines. Kinetic coefficients $k^+_{BA} =$ 10 a.u., $k^-_{CA} = 16$ a.u., composition of aqueous solution $y_C = 0.4$. The dashed line corresponds to the case of infinitely high growth rate $D_\infty = k^+_{BA}/k^+_{CA} = 0.625$.

growth rate unambiguously–additional information on the solid solution composition is required.

Note, that the growth rate depends not only on the supersaturation, but also on the solid solution composition and the kinetic coefficients. If the kinetic coefficients for the end members differ strongly, quite a slight variation in a crystal composition can significantly increase/decrease the growth rate. To illustrate this we have performed model calculations for the series $(Cu,Ni)(NH_4)_2(SO_4)_2 \cdot 6H_2O$. Using the data on solubilities and kinetic coefficients of the Cu and Ni end members from the paper by Kuschel and others (1982) we estimated effect of the crystal composition on the growth rate. In accordance with equation (41) it was shown that since $k^+_{Cu\text{-}salt}K_{Cu\text{-}salt} \gg k^+_{Ni\text{-}salt}K_{Ni\text{-}salt}$ incorporation of only $x_{Co} = 0.01$ into the nickel end member three times increases its growth rate. However, due to the same reason incorporation of even $x_{Ni} =$ 0.10 into the cobalt end member does not change its growth rate significantly. This phenomenon might be also responsible for effect of the Sr impurity on the calcite growth rate (Wasylenki and others, 2005). The authors reported that the small additions of Sr into the mother solution (so that $x_{Sr} < 0.01$) increased the calcite growth rate, in some cases up to two times. Such strong acceleration of the growth rate might result from the differences in kinetic coefficients. Unfortunately, we do not have necessary experimental data to verify this hypothesis.

CHEMICAL INTERACTION WITH THE SUBSTRATE

Let us consider now a very common case of an aqueous solution of the composition y_C (point 1 in fig. 1) contacting with a substrate (seed crystal) of the composition $1 - x_{BAs} = x_{CAs} \neq x_{CA}$ (point 4 in fig. 1). In this case the equations (37) and (38) should be replaced with

$$J_{BA} = k^+_{BA}(y_B\Sigma\Pi - K_{BA}f_{BAs}x_{BAs}) \quad (42)$$

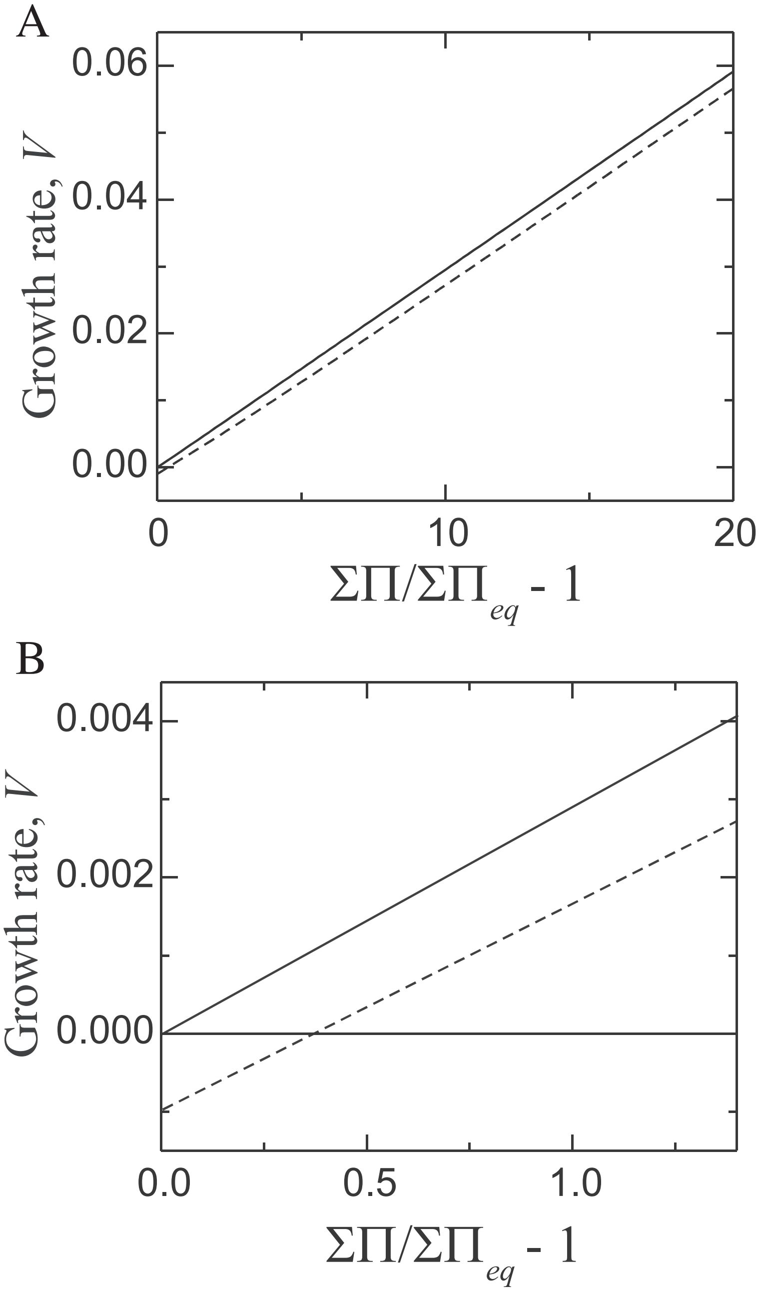

Fig. 4. (A) Growth rate V (a.u.) as a function of supersaturation $\Sigma\Pi/\Sigma\Pi_{eq} - 1$ for the system shown in figure 1. Solid line–stress free crystallization, dashed line–crystallization on the substrate of different composition, the value of misfit $(b_{BA} - b_{CA})/b_s = 0.04$; for other numerical values see figures 1 and 3. (B) Enlarged part of the plot shown in figure 4A close to the equilibrium state. The quasi-equilibrium between the strained solid solution and the aqueous solution is attained at $\Sigma\Pi/\Sigma\Pi_{eq} - 1 = 0.359$, where $\Sigma\Pi_{eq}$ is calculated from the equilibrium phase diagram (fig. 1).

$$J_{\mathrm{CA}} = k^{+}_{\mathrm{CA}}(y_{\mathrm{C}}\Sigma\Pi - K_{\mathrm{CA}} f_{\mathrm{CA}s} x_{\mathrm{CA}s}) \tag{43}$$

The total flux of each component is equal to zero $J_{i\mathrm{A}} = 0$ ($i = \mathrm{B, C}$) if conditions $y_i\Sigma\Pi = K_{i\mathrm{A}} f_{i\mathrm{A}s} x_{i\mathrm{A}s}$ are held. These two mutually independent conditions already considered above [see equations (19) and (20)] divide the phase space into four different regions (fig. 2). In the Lippmann diagram the lines, which bound these regions, represent hyperbolas [equations (19) and (20), fig. 2]. Each of them describes equilibrium of a given solid solution with a series of aqueous solutions with respect to one individual component. For $y_i = 1$ the solubility products $\Sigma\Pi$ take on a values $K_{i\mathrm{A}} f_{i\mathrm{A}s} x_{i\mathrm{A}} < \Sigma\Pi_{eq} = K_{i\mathrm{A}}$, that is the lines $\Sigma\Pi(y_i)$ intersects the ordinate axis lower than the solutus curve does. Compared with the saturation curves for pure end member solids (Glynn and Reardon, 1990; Glynn and others, 1990; Glynn, 2000) these lines have the same meaning, however, the saturation curves for pure end member solids express the equilibrium conditions only for the end members ($x_{i\mathrm{A}} = 1$) placed in a contact with a given solution y_i, whereas our lines described by equations (19) and (20) consider equilibrium conditions for any particular solid solution. Since the values of $x_{i\mathrm{A}s}$ are independent of y_i and $J_{i\mathrm{A}}$, the equation (39) is no longer valid, and the four different cases should be considered in accordance with (42) and (43).

If $J_{\mathrm{BA}} > 0$ and $J_{\mathrm{CA}} > 0$ (region I in fig. 2), the crystal growth occurs. After the deposition of a few initial elementary layers the original substrate is completely covered by deposited substance and does not affect the process any more. The crystal assumes the stationary composition $x_{i\mathrm{A}s} \to x_{i\mathrm{A}}$. The growth kinetics is described by the equations (37) to (40) and the fluxes change by the values of $k^{+}_{i\mathrm{A}} K_{i\mathrm{A}}(f_{i\mathrm{A}} x_{i\mathrm{A}} - f_{i\mathrm{A}s} x_{i\mathrm{A}s})$.

In the opposite case $J_{\mathrm{BA}} < 0$ and $J_{\mathrm{CA}} < 0$ (region III in fig. 2) the crystal dissolves *congruently*, and its dissolution rate is completely determined by that component of the solid solution, which would have the highest dissolution rate $V \approx -w \cdot \max(J_{\mathrm{BA}}, J_{\mathrm{CA}})$ when taken as an individual component. The sign "$-$" reflects the fact that both fluxes are negative and the dissolution rate is expected to take on a positive value. Indeed, the driving forces and resulted fluxes should be different for components BA and CA, however, the crystal can dissolve *only as a whole*. Therefore, the dissolution rate will be controlled by that component, which has the fastest detachment rate. This estimate ignores the mutual influence of fluxes, which can somehow affect the net dissolution process. Considering such more complicated interactions is beyond the scope of the paper, our aim here is to show the system behavior depending on the aqueous and solid solution compositions. This process is directed towards the stoichiometric saturation state (Glynn and others, 1990; Glynn and Reardon, 1990, 1992; Glynn, 2000) described above and illustrated in figure 2. However, before the stoichiometric saturation state is achieved the aqueous solution passes the region where the replacement reactions may occur ($J_{\mathrm{BA}} > 0, J_{\mathrm{CA}} < 0$ or $J_{\mathrm{BA}} < 0, J_{\mathrm{CA}} > 0$: regions II and IV in fig. 2, respectively).

Let us consider the crystal of composition $x_{\mathrm{C}s}$ placed in the initial solution T0 (pure water) and follow the dissolution pathway (in this section we assume that the crystal is large compared with the solution volume and the aqueous solution changes its composition in the course of the crystal dissolution). Between points T0 and T1 the crystal dissolves congruently and no replacement reaction takes place (fig. 2). At the point T1 the equilibrium is achieved for the component BA, but the component CA should continue to dissolve and the solution comes to the region II in figure 2, where the coupled dissolution-precipitation reaction may occur. This point has a rather theoretical meaning because in the course of real dissolution process the replacement reaction has a low probability. The replacement seems unlikely to proceed at the atomic level, because such a mechanism would require anomalous high diffusion rate in solid and the process should stop after a few elementary layers have been replaced. Significant replacement rates are only possible if the substrate has a high degree of porosity or if the molar volumes of the substrate and the deposit are considerably different. The quasi-equilibrium state (replacement within a small number of monatomic layers prevents further interaction between the crystal and the solution) may take place - only if the dissolution rate is very low either due to the closeness to the true equilibrium point or for some other reason. In other cases the crystal should dissolve without re-precipitation with the dissolution rate $V \approx -wJ_{CA}$.

Further congruent dissolution leads to the point T2 (fig. 2), where the system achieves the *primary saturation state* (Glynn and Reardon, 1990, 1992; Glynn, 2000). The aqueous solution remains undersaturated with respect to one of the considered solid solution components, and the dissolution continues. At the same time the aqueous solution becomes supersaturated with respect to other solid solution T2' that may result in simultaneous precipitation at some localities not far from the original crystal or even immediately on the dissolving surface. Such coupled reactions of dissolution and precipitation were frequently observed in experiments (Glikin and Sinai, 1983; Bolkhovityanov, 1990; Kuzmina and others, 1994; Glikin, 1995; Kryuchkova and others, 2002; Putnis, 2002; Glikin and others, 2003; Voloshin and others, 2003a, 2003b; Putnis and Mezger, 2004).

Finally, if no re-precipitation occurs for some reason, for example because of high energy barrier, the system can attain the quasi-equilibrium stoichiometric saturation state (point T3 in fig. 2).

Thus, despite the numerous theoretical possibilities only two processes should usually occur at a micro scale (the system is large enough to avoid considering the elementary attachment/detachment processes and the surface morphology but small enough to not take into account diffusion and stirring in the solution): (1) growth of crystal with a composition and growth rate defined *solely* by a solution and (2) congruent dissolution whose rate is controlled by both phases - crystal and solution. The first opportunity corresponds to the field I in figure 2, whereas the second one refers to three other fields. The replacement reactions are possible and are observed in experiment (Glikin and Sinai, 1983; Bolkhovityanov, 1990; Kuzmina and others, 1994; Glikin, 1995; Kryuchkova and others, 2002; Putnis, 2002; Glikin and others, 2003; Voloshin and others, 2003a, 2003b; Putnis and Mezger, 2004) but usually need the mass transport that complicates the problem significantly and are not considered here.

SUPERSATURATION

At this point the important question needs to be answered: how the supersaturation of a given aqueous solution with respect to a given solid solution can be defined. Some of such definitions were elaborated in Prieto and others(1993) and Astilleros and others (2003a), but they are not satisfactory in our point of view.

The first approach suggests that supersaturation is a *thermodynamic* variable, which corresponds to deviation of the given aqueous solution from the equilibrium state (namely the aqueous solution, which is in equilibrium with the crystal growing from the given solution). It is self-evident that this supersaturation is independent of the substrate composition and even of its presence and any solution can be characterized by one and only *one* value of supersaturation. Due to the proportionality between growth rate and supersaturation, this concept is widely used in study of crystallization kinetics. Such a supersaturation was introduced in the section "crystal growth: thermodynamic approach" for the systems, which are close to equilibrium, and according to the equation (29) it is equal to $\xi = \Delta\mu_{BA}/RT = \Delta\mu_{CA}/RT$.

The second approach is aimed to find the driving force for crystallization/dissolution of given substrate crystal placed into given aqueous solution. It is clear that the supersaturation should be a function of two independent differences in chemical potentials of both components between aqueous solution and solid solution $\Delta\mu_{BA}/RT$ and $\Delta\mu_{CA}/RT$ defined in the equations (23) and (24), respectively.

In the paper by Astilleros and others (2003a) the supersaturation ξ was introduced in the form of two functions δ_{BA} and δ_A calculated as follows

$$\delta_{BA}(x_{BA}) = \frac{a_B a_A}{f_{BA} x_{BA} K_{BA}} \tag{44}$$

$$\delta_{CA}(x_{CA}) = \frac{a_C a_A}{f_{CA} x_{CA} K_{CA}} \tag{45}$$

where the crystal growth is supposed to be controlled by the minimal values of $\delta_{iA}\ (x_{iA})$ $(i = \mathrm{B, C})$. It is easy to show that not far from the equilibrium $\Delta\mu_{iA}/RT = \ln(a_i a_A / f_{iA} x_{iA} K_{iA}) \approx a_i a_A / f_{iA} x_{iA} K_{iA} - 1 = \delta_{iA}(x_{iA}) - 1$ and thus the supersaturation ξ is approximately equal to $\xi \approx \min(\Delta\mu_{BA}/RT + 1, \Delta\mu_{CA}/RT + 1)$. The physical meaning of the variable is that although the fluxes of two components are mutually independent the crystal cannot grow "with two different rates" and the slowest flux should define deviation from the equilibrium and, correspondingly, the growth rate. So in this case the slowest flux plays a role of a "limitation stage" of crystallization. On the other hand, this expression is valid only in a first approximation, since the mutual influence of the fluxes cannot be excluded and to calculate the supersaturation accurately a more rigorous approach is necessary. This expression is also applicable for the dissolution and replacement reactions. The dissolution is controlled by that component, which has the maximal detachment rate, and hence it is characterized by the maximal negative value of corresponding flux.

Another approach to definition of supersaturation starts from the net reaction (1) and finds the difference between the free energy of given solid solution and aqueous solution $\Delta G = x_{BA}\Delta\mu_{BA} + x_{CA}\Delta\mu_{CA}$, where the differences in chemical potentials are found from the equations (23) and (24). This concept based on the stoichiometric saturation state was suggested by M. Prieto and co-workers (1993) and in our notations resulted in the following expression

$$\beta(x_{BA}) = \left(\frac{a_B a_A}{f_{BA} x_{BA} K_{BA}}\right)^{x_{BA}} \left(\frac{a_C a_A}{f_{CA} x_{CA} K_{CA}}\right)^{x_{CA}} = [\delta_{BA}(x_{BA})]^{x_{BA}}[\delta_{CA}(x_{CA})]^{x_{CA}} \tag{46}$$

This function has a physical meaning only for the dissolution near to the stoichiometric saturation state and, therefore, cannot be used for the most aqueous solution–solid solution systems.

In our opinion, no universal single variable can be found, which would characterize the supersaturation (undersaturation) in general case, since two independent chemical potential differences $\Delta\mu_{BA}$ and $\Delta\mu_{CA}$ govern the attachment/detachment processes. Yet in any particular case it is certainly possible to find the single value, which control the growth/dissolution process. It should be emphasized that the supersaturation cannot be determined *a priori* from the composition of aqueous solution alone, like it is normally done for one-component solids. The composition of growing crystal must also be taken into account, which can be found by solving the set of equations (37) to (39).

Application of the supersaturation concept also needs to take into account the differences between relative and absolute supersaturations. Introduction of supersaturation (driving force of some growth/dissolution process) is always aimed to predict or at least estimate the rate of the corresponding process, since in general the rate of some reaction is a product of the driving force and some constant called by kinetic coefficient (Prigogine and Defay, 1954). For our case this relationship can get two forms: $J_{iA} = \mathrm{const}\cdot\Delta\mu_{iA}/RT = \mathrm{const}\cdot\ln(a_i a_A / a_{ieq} a_{Aeq})$ deduced from postulates of the chemical thermodynamics - see equations (27) to (29) and $J_{iA} = k_{iA}^{+}(a_i a_A - a_{ieq} a_{Aeq})$, which directly results from equations (37) and (38) obtained from equations of the chemical kinetics. Respectively, the former case considers dimensionless or *relative* supersaturation $\xi = \ln (a_i a_A / a_{ieq} a_{Aeq})$, whereas the later one introduces *absolute* supersaturation $a_i a_A - a_{ieq} a_{Aeq}$. These two forms are fully equivalent to each other as long as deviations from equilibrium are slight and $\ln (a_i a_A / a_{ieq} a_{Aeq}) \approx (a_i a_A - a_{ieq} a_{Aeq} / a_{ieq} a_{Aeq})$. However, for the wide range of growth conditions (especially strongly non-equilibrium ones) the use of the *absolute* supersaturation/undersaturation seems to be more appropriate. For example, the crystal CA will obviously dissolve in the solution containing only the B^{n+} and A^{n-} ions with the *finite* rate $V = wk^+_{CA}(0 - K_{CA}) = -wk^+_{CA}K_{CA}$ [see equation (38)], whereas with the use of relative undersaturation the *infinitely high* dissolution rate is predicted $V = wk^+_{CA}K_{CA} \ln (0/K_{CA}) \rightarrow -\infty$ [see equation (41)].

EFFECT OF MISFIT STRAIN

In the previous section it was presumed that the substrate no longer affects the crystal growth after a few monolayers have been deposited. Experiments, however, show strong effect of substrate on the growth kinetics (Bolkhovityanov, 1982; Ristic and others, 1997; Moshkin and others, 2000; Astilleros and others, 2003b). The main factor responsible for such a behavior is the action of misfit strain–the effect routinely observed in the processes of semiconductor heteroepitaxial film growth–see, for example, (Pimpinelli and Villain, 1998; Kaganer and Ploog, 2001) and studied insufficiently for solution grown crystals.

Let us consider a series of monolayers deposited on a substrate of considerable thickness and surface area (labeled by subscript $_s$). For definiteness, let the substrate be the (001) face of a cubic crystal. The plane deformation problem of elasticity is well known (Elsen and Ettenberg, 1978) and for a thick substrate has a simple solution. The components of the strain tensor ε_j in the layer, which has the lattice constant b, are expressed as

$$\varepsilon_j = \begin{cases} \dfrac{b - b_s}{b_s} & j = 1, 2 \\ 0 & j = 3, \ldots 6 \end{cases} \tag{47}$$

The components of the stress tensor σ_j have a form

$$\sigma_j = \begin{cases} \dfrac{E}{1 - \nu}\left(\dfrac{b - b_s}{b_s}\right) & j = 1, 2 \\ \dfrac{2\nu E}{1 - \nu}\left(\dfrac{b - b_s}{b_s}\right) & j = 3 \\ 0 & j = 4, \ldots 6 \end{cases} \tag{48}$$

where E is the Young modulus, ν is the Poisson ratio. It is important to note that the stress (strain) in each layer only depends on the difference in lattice constants between the layer and the substrate, so the deposited layers do not affect each other, and the stress in the substrate is equal to zero. Let us assume that the lattice constant obeys the Vegard's rule $b = x_{BA} b_{BA} + x_{CA} b_{CA}$, where b_{BA} and b_{CA} are the lattice constants of the end members of the series. Thus $b - b_s = (b_{BA} - b_{CA})(x_{BA} - x_{BAs})$. The elastic energy U of the solid (per one mole) is expressed via general equation (Landau and Lifshitz, 1970)

$$U = \frac{w}{2} \sum_{j=1}^{6} \sigma_j \varepsilon_j \tag{49}$$

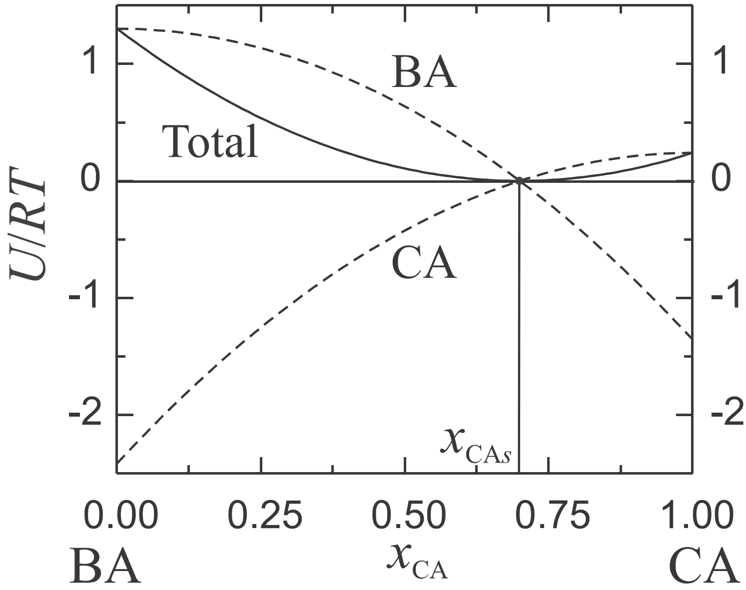

Fig. 5. Elastic energy U/RT of solid solution deposited on the substrate of composition $x_{CAs} = 0.7$ (solid line), and the partial values related to components BA and CA (dashed lines). The temperature is $T = 25$ °C, elastic constant $E/(1-v) = 10^{11}$ N/m^2, misfit $(b_{BA} - b_{CA})/b_s = 0.04$, molar volume $w = 40$ cm^3/mol.

Here w is the molar volume. Substituting expressions (47) and (48) into (49) gives

$$U = \frac{Ew}{1-\nu}\left(\frac{b_{BA} - b_{CA}}{b_s}\right)^2 (x_{BA} - x_{BAs})^2 \tag{50}$$

The molar elastic energy U characterizes the solid solution as a whole. However, like the other mean molar values, it can be represented as a sum of two partial values related to the components BA and CA: $U = x_{BA}U_{BA} + x_{CA}U_{CA}$ (fig. 5), where

$$U_{BA} = U + (1 - x_{BA})\frac{\partial U}{\partial x_{BA}} \tag{51}$$

$$U_{CA} = U - x_{BA}\frac{\partial U}{\partial x_{BA}} \tag{52}$$

Taking the elastic stress into account the chemical potentials of the components BA and CA in the growing layer should be increased by the values U_{BA} and U_{CA}, respectively. In equilibrium

$$\Delta\mu_{BA} = \mu_B^{eq} + \mu_A^{eq} - \mu_{BA}^{ss} - U_{BA} = RT\ln\left(\frac{a_B a_A}{f_{BA}x_{BA}}\right) - \Delta\mu_{BA}^0 - U_{BA} = 0 \tag{53}$$

$$\Delta\mu_{CA} = \mu_C^{aq} + \mu_A^{aq} - \mu_{CA}^{ss} - U_{CA} = RT\ln\left(\frac{a_C a_A}{f_{CA}x_{CA}}\right) - \Delta\mu_{CA}^0 - U_{CA} = 0 \tag{54}$$

After a rearrangement of the equations (53) and (54) one can obtain the expressions for the solubility product (additional subscript U denotes the presence of misfit stress)

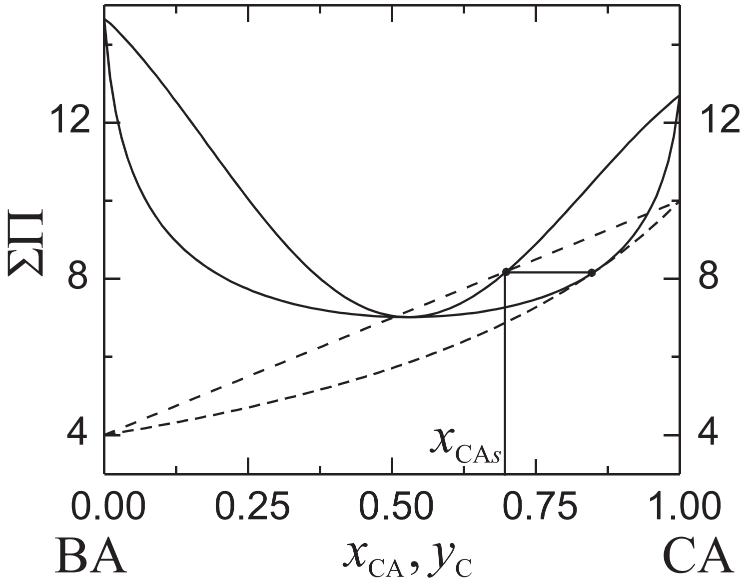

Fig. 6. Lippmann diagram for the system shown in figure 1, where the solid solution crystallizes on the substrate of composition $x_{CAs} = 0.7$ (solid lines); the conventional equilibrium phase diagram is shown with dashed lines. The straight solid line connects the points, for which the elastic strain is absent. The elastic energy of the system is represented in figure 5.

$$a_{BeqU}a_{AeqU} = f_{BA}K_{BA}x_{BA} \exp\left(\frac{U_{BA}}{RT}\right) \tag{55}$$

$$a_{CeqU}a_{AeqU} = f_{CA}K_{CA}x_{CA} \exp\left(\frac{U_{CA}}{RT}\right) \tag{56}$$

Equations (55) and (56) define the quasi-equilibrium phase diagram. If the equilibrium solid solution and the substrate have the same composition and no stress occurs (fig. 6), the quasi-equilibrium and the true equilibrium phase diagram coincide. The elastic energy U is always positive but the partial values U_{BA} and U_{CA} have the opposite signs (fig. 5). Division of equation (56) by equation (55) directly gives the value of distribution coefficient in the presence of stress

$$D_{eqU} = D_{eq} \exp\left(\frac{U_{CA} - U_{BA}}{RT}\right) = D_{eq} \exp\left(-\frac{1}{RT}\frac{\partial U}{\partial x_{BA}}\right) \tag{57}$$

where the equilibrium distribution coefficient in the absence of stress can be found from equation (17). The effect of stress on the crystal composition was calculated in a similar way by Yu. B. Bolkhovityanov (1982) for the liquid phase epitaxy grown semiconductor $A^{III}B^{V}$ compounds like Ga(As,P) and by S. V. Moshkin and co-workers (2000) for the mixed K-Rb dihydrogen phthalate crystals. In both papers a satisfactory agreement between the theory and experiment was found. For example, in the paper (Moshkin and others, 2000) solid solutions of potassium and rubidium dihydrogen phthalate $(K,Rb)C_8H_5O_4$ were grown on $KC_8H_5O_4$ seed crystals and without seed crystals. For the spontaneous nucleated crystals the distribution coefficients were found to be constant and independent of the Rb fraction in aqueous solution [as stated by equation (18) for the systems with nearly ideal solid solutions]. For the seeded

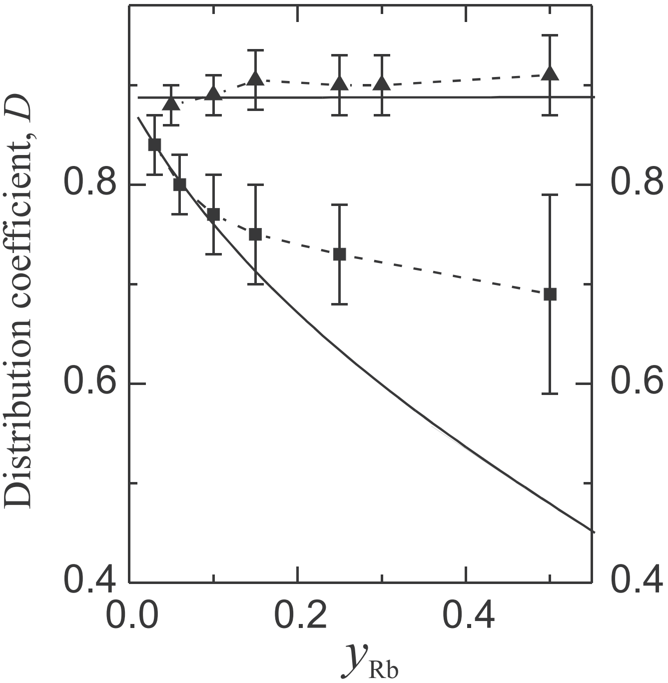

Fig. 7. Distribution coefficient D for the solid solutions of K and Rb dihydrogen phthalate (K,Rb)$C_8H_5O_4$ as a function of Rb fraction in a solution y_{Rb} [after Moshkin and others (2000)]. Points and dashed lines represent experimental data: triangles–spontaneous nucleation of crystals, squares–growth on $KC_8H_5O_4$ seed crystals. Solid lines–theoretical calculations for unseeded (no stress, upper line) and seeded (with stress, lower line) crystals. Relative strong discrepancies between theory and experiment at high y_{Rb} (lattice misfit is high) result from the plastic stress relaxation during crystal growth.

crystals, however, the distribution coefficient changed significantly as the Rb fraction in aqueous solution increased. These changes agreed well with theoretical predictions (57) (fig. 7).

The fluxes of components into the crystal can be obtained after minor modifications to the equations (37) and (38):

$$J_{BA} = k^{+}_{BA}\left(y_B \Sigma\Pi - K_{BA} f_{BA} x_{BA} \exp\left(\frac{U_{BA}}{RT} \right) \right) \tag{58}$$

$$J_{CA} = k^{+}_{CA}\left(y_C \Sigma\Pi - K_{CA} f_{CA} x_{CA} \exp\left(\frac{U_{CA}}{RT} \right) \right) \tag{59}$$

The changes in the incorporation fluxes are mainly restricted by the shift of phase equilibria (fig. 4), so the zero supersaturation expressed in usual notations $\Sigma\Pi/\Sigma\Pi_{eq} - 1 = 0$ is accompanied by crystal dissolution. The equilibrium state requires higher activity product of the ions in aqueous solution, which can be calculated numerically from the equation (58) or (59). In a wide range of supersaturations the kinetic curves are approximated with straight lines of similar slope. The same effect of elastic strain on the growth kinetics was observed experimentally for the $NaClO_3$ crystals (Ristic and others, 1997). Using synchrotron radiation the authors induced a small strongly strained area on the surface of $NaClO_3$ crystal and then measured growth and dissolution rates over the crystal surface. On the non-irradiated (non-strained) areas the zero growth/dissolution rates were observed for zero supersaturation as predicted by classic crystal growth theories. However, on the irradiated (strained) area at the zero supersaturation the crystal dissolved. The zero growth rate was observed for non-zero supersaturation equal to 0.32 and the corresponding growth as well as dissolution curves $V(\xi)$ were shifted along the abscissa axis without change of slope. This shift is likely to be related to increase the crystal free energy due to the strain action.

The effect of supersaturation on the distribution coefficient for crystals with mismatch stress is very close to the case of stress free crystal but the equilibrium distribution coefficient can have another value (fig. 3).

It is worth noting that this simple description is valid for the steady growth, when several first monolayers have been already deposited and interface effects are negligible. The growth of first layers can drastically differ from the predictions made and from the growth of successive layers (Astilleros and others, 2003b; Sánchez-Pastor and others, 2005; Shtukenberg and others, 2005). For example, the growth rate of the first layer of $BaCrO_4$ on the $BaSO_4$ substrate is several times higher than the growth rate of the second $BaCrO_4$ layer on the first $BaCrO_4$ layer (Astilleros and others, 2003b; Shtukenberg and others, 2005). The main reason for such behavior is the surface relaxation phenomena or formation of wetting layer on the substrate that reduces the internal stress due to "non-elastic" deformation of the first layer (Pimpinelli and Villain, 1998; Astilleros and others, 2003b; Shtukenberg and others, 2005). Furthermore, nanoscale observations show that such heteroepitaxial growth can be accompanied by formation of 3D islands and ripples. Due to significant free area the surface roughness arisen reduces elastic stress (Pimpinelli and Villain, 1998; Lea and others, 2003; Sánchez-Pastor and others, 2005; Shtukenberg and others, 2005) and affects the growth kinetics. Evolution of the islands with a time (for example, their coalescence and formation of the flat surface) certainly should affect the growth kinetics as well. The discussion of these phenomena is far beyond the scope of the paper, since here we give only a phenomenological approach, which suits for the steady growth and does not involve atomic scale mechanisms.

CONCLUSION

The presented theory describes the aqueous solution - solid solution equilibria and quasi-equilibria as well as heterogeneous chemical kinetics on a simple and clear thermodynamical basis. The model is applicable to the relatively narrow class of solid solution - aqueous solution systems and has the phenomenological character, that is, it does not deal with microscopic processes, and instead it uses macroscopic parameters known from experiment. Within these restrictions the model is able to predict the growth/dissolution rates of any seed crystal placed into any aqueous solution. We believe that this model could be easily applied to the simple systems like $(Ba,Sr)SO_4$-H_2O. Successful calculations for the complex natural systems require further development of the model and also some additional experimental data on the elementary processes in the systems. At this moment we cannot verify most of the theoretical results obtained due to the lack of experimental data. Therefore, a detailed experimental study of crystallization kinetics in SS-AS systems can be considered as the necessary step in developing this approach.

ACKNOWLEDGMENTS

The work is supported by Russian Foundation for Basic Research RFBR (project 05-05-64289). The authors also would like to thank P. Glynn and anonymous reviewers for their valuable comments and suggestions.

References

Astilleros, J. M., Pina, C. M., Fernández-Díaz, L., and Putnis, A., 2003a, Supersaturation functions in binary solid solution-aqueous solution systems: Geochimica et Cosmochimica Acta, v. 67, p. 1601–1608.

——— 2003b, Nanoscale growth of solids crystallising from multicomponent aqueous solutions: Surface Science, v. 545, p. L767-L773.

Azimov, P. Ya., and Shtukenberg, A. G., 2000, Simulation of phase diagrams for water-salt systems with solid solutions: Russian Journal of Inorganic Chemistry, v. 45, p. 1302–1309.

Bolkhovityanov, Yu. B., 1982, The contact phenomena between the liquid phase and the substrate during LPE of A^3B^5 compounds: Journal of Crystal Growth, v. 57, p. 84–90.

——— 1990, Common mechanism of relaxation of non-equilibrium liquid-solid interface before liquid-phase heteroepitaxy of $A^{III}B^{V}$ compounds, *in* Sheftal N. N., editor, Growth of Crystals: Moscow, Nauka, v. 18, p. 158–172.

Chernov, A. A., 1970, Growth of co-polymer chains and mixed crystals: tests and failures statistics: Uspekhi Phyzicheskih Nauk, v. 100, N 2, p. 277–328 (in Russian).

——— 1984, Modern Crystallography III: Crystal Growth: Berlin, Springer Verlag, 517 p.

Chernov, A. A., and Malkin, A. I., 1988, Regular and irregular growth and dissolution of (101) ADP faces under low supersaturation: Journal of Crystal Growth, v. 92, p. 432–444.

Chernov, A. A., Rashkovich, L. N., and Mkrtchyan, A.A., 1987, Optical interference investigation of surface processes of growth of crystals of KDP, DKDP, and ADP: Soviet Physics Crystallography, v. 32, p. 432–442.

Davis, K. J., Dove, P. M., and De Yoreo, J. J., 2000, The role of Mg^{2+} as an impurity in calcite growth: Science, v. 290, p. 1134–1137.

Elsen, G. H., and Ettenberg, M., 1978, Synthesis of $A^{III}B^{V}$ heteroepitaxial structures, *in* Goodman, C. H. L., editor, Crystal growth. Theory and techniques: New York, London, Plenum Press, v. 2, p. 9–76.

Ghiorso, M. S., 1994, Algorithms for the estimation of phase stability in heterogeneous thermodynamic systems: Geochimica et Cosmochimica Acta, v. 58, p. 5489–5501.

Glikin, A. E., 1995, To a theory of isomorphic mixed-crystal formation: Zapiski Vserossiiskogo Mineralogicheskogo Obschestva, v. 124, N 5, p. 125–134 (in Russian).

——— 1996, On equilibrium supercooled solutions in connection with isomorphic mixed-crystal formation: Zapiski Vserossiiskogo Mineralogicheskogo Obschestva, v. 125, N 5, p. 103–111 (in Russian).

Glikin, A. E., and Sinai, M. Yu., 1983, Experimental investigation of monocrystal pseudomorph formation: Zapiski Vserossiiskogo Mineralogicheskogo Obschestva, v. 112, N 6, p. 742–748 (in Russian).

Glikin, A. E., Kovalev, S. I., Rudneva, E. B., Kryuchkova, L. Yu., and Voloshin, A. E., 2003, Phenomena and mechanisms of mixed crystal formation in solutions I. General concept on the example of the system $KHC_8H_4O_4$-$RbHC_8H_4O_4$-H_2O: Journal of Crystal Growth, v. 255, p. 150–162.

Glynn, P., 2000, Solid-solution solubilities and thermodynamics: Sulfates, carbonates and halides, *in* Alpers, Ch. N., Jambor, J. L., and Nordstrom, D. K., editors, Sulfate minerals: Crystallography, Geochemistry and Environmental Significance: Mineralogical Society of America Reviews in Mineralogy and Geochemistry, v. 40, p. 480–511.

Glynn, P. D., and Reardon, E. J., 1990, Solid-solution aqueous-solution equilibria: Thermodynamic theory and representation: American Journal of Science, v. 290, p. 164–201.

——— 1992, Reply to a comment by Königsberger, E., and Gämsjager, H., On "Solid-solution aqueous-solution equilibria: Thermodynamic theory and representation": American Journal of Science, v. 292, p. 215–225.

Glynn, P. D., Reardon, E. L., Plummer, L. N., and Busenberg, E., 1990, Reaction path and equilibrium end-points in solid-solution aqueous-solution systems: Geochimica et Cosmochimica Acta, v. 54, p. 267–282.

Henderson, L. M., and Kracek, F. C., 1927, The fractional precipitation of barium and radium chromates: Journal of American Chemical Society, v. 49, p. 738–749.

Kaganer, V. M., and Ploog, K. H., 2001, Energies of strained vicinal surfaces and strained islands: Physical Review B, v. 64, p. 205301–205315.

Kamenetskaya, D. C., 1968, On the nucleation in supercooled liquids, *in* Sheftal, N. N., editor, Growth of Crystals, v. 8: Moscow, Nauka, p. 328–333.

Kasatkin, I. A., Glikin, A. E., Bradaczek, H., and Franke, W., 1995, Kinetics of mixed crystal $K_2(SO_4,CrO_4)$ growth from aqueous solution: Crystal Research and Technologies, v. 30, p. 659–666.

Kryuchkova, L. Yu., Glikin, A. E., Voloshin, A. E., and Kovalev, S. I., 2002, Kinetic-morphological phenomena of mixed crystal growth and isomorphic replacement in solutions (on the example of the series $(Co,Ni)(NH_4)_2(SO_4)_2{\cdot}6H_2O$): Zapiski Vserossiiskogo Mineralogicheskogo Obschestva, v. 131, N 3, p. 62–77 (in Russian).

Kuschel, F., König, A. N., and Gropp, R., 1982, Crystal growth in magnetic field (I). Crystallization of $Me(NH_4)_2(SO_4)_2 \cdot 6H_2O$ (Me = Zn, Cu, Ni, Fe) from aqueous solutions in moderate magnetic fields: Crystal Research and Technologies, v. 17, p. 793–799.

Kuzmina, M. A., Moshkin, S. V., Boldyreva, O. M., and Shakhverdova, I. P., 1994, Formation of defects during growth of potassium-rubidium hydrogen phtalate crystals with artificial zoning, *in* Smirnov, Yu. M., editor, Physics of crystallization: Tver, Tver University Press, p. 103–115 (in Russian).

Landau, L. D., and Lifshitz, E. M., 1970, Theory of Elasticity: Oxford, Pergamon Press, 160 p.

Lasaga, A., 1981, Rate laws of chemical reactions, *in* Lasaga, A. C., and Kirkpatrick, R. J., editors, Kinetics of Geochemical Processes: Mineralogical Society of America Reviews in Mineralogy, v. 8, p. 1–68.

Lea, A. S., Hurt, T. T., El-Azab, A., Amonette, J. E., and Baer, D. R., 2003, Heteroepitaxial growth of a manganese carbonate secondary nano-phase on the (1014) surface of calcite in solution: Surface Science, v. 524, p. 63–77.

Lippmann, F., 1980, Phase diagrams depicting the aqueous solubility of mineral systems: Neues Jahrbuch für Mineralogie, Abhandlungen, v. 139, N 1, p. 1–25.

Moshkin, S. V., Kuz'mina, M. A., Boldyreva, O. M., and Ivanova, T. I., 2000, Growth of mixed crystals under the nonstationary conditions. 1. Equilibria and quasiequilibria: Crystallography Reports, v. 45, p. 1041–1046.

Mullin, J. W., and Kitamura, M., 1985, The crystallization and co-crystallization of ammonium and potassium aluminium sulphates from aqueous solution: Journal of Crystal Growth, v. 71, p. 118–124.

Pimpinelli, A., and Villain, J., 1998, Physics of crystal growth: Cambridge, Cambridge University Press, 377 p.

Prieto, M., Putnis, A., and Fernández-Díaz, L., 1993, Crystallization of solid solutions from aqueous solutions in a porous medium: Zoning in (Ba, Sr)SO_4: Geological Magazine, v. 130, p. 289–299.

Prigogine, I., and Defay, R., 1954, Chemical Thermodynamics: London, Longmans, Green and Company Limited, 543 p.

Putnis, A., 2002, Mineral replacement reactions: from macroscopic observations to microscopic mechanisms: Mineralogical Magazine, v. 66, p. 689–708.

Putnis, C. V., and Mezger, K., 2004, A mechanism of mineral replacement: Isotope tracing in the model system KCl-KBr-H_2O: Geochimica et Cosmochimica Acta, v. 68, p. 2839–2848.

Ratner, A. P., 1933, On the theory of electrolyte distribution between crystalline and liquid phase: Trudi RIAN, v. 2, p. 67–73 (in Russian).

Ristic, R. I., Shekunov, B. Yu., and Sherwood, J. N., 1997, The influence of synchrotron radiation-induced strain on the growth and dissolution of brittle and ductile materials: Journal of Crystal Growth, v. 179, p. 205–212.

Sally, I.V., 1963, Physical fundamentals of the alloy structure formation: Moscow, Metallurgizdat, 265 p.

Sánchez-Pastor, N., Pina, C. M., Astilleros, J. M., Fernández-Díaz, L., and Putnis, A., 2005, Epitaxial growth of celestite on barite (001) face at a molecular scale: Surface Science, v. 581, p. 225–235.

Shtukenberg, A. G., and Azimov, P. Ya., 2001, Inclusion of the aqueous solution nonideality into the calculation of phase diagrams for systems of water with salts that form complete solid solutions: Russian Journal of Inorganic Chemistry, v. 46, p. 1596–1599.

Shtukenberg, A. G., Astilleros, J. M., and Putnis, A., 2005, Nanoscale observations of epitaxial growth of hashemite on barite (001): Surface Science, v. 590, p. 212–223.

Soloviev, V., Shtukenberg, A., Punin, Yu., and Azimov, P., 1997, Study of mixed crystal growth kinetics: Proceedings of Fifth International Symposium on Hydrothermal Reactions (Gatlinburg, Tennessee, USA, July 20–24 1997), p. 267–268.

Temkin, D. E., 1980, Kinetic conditions on the growth front of the mixed crystal, *in* Sheftal N. N., editor, Growth of Crystals: Moscow, Nauka, v. 13, p. 134–142.

——— 1981, Interface kinetics in the growth of two-component crystals: Journal of Crystal Growth, v. 52, p. 299–301.

Thorstenson, D. C., and Plummer, L. N., 1977, Equilibrium criteria for two-component solid reacting with fixed composition in aqueous phase: American Journal of Science, v. 277, p. 1203–1223.

Treivus, E. B., 2000, On the isotermic diagrams of ternary systems containing binary solid solutions: Bulletin of the St. Petersburg State University, Series 7, Part 2, N 15, p. 14–23 (in Russian).

Tsuchiyama, A., Kitamura, M., and Sunagawa, I., 1981, Distribution of elements in growth of (Ba,Pb)$(NO_3)_2$ crystals from the aqueous solution: Journal of Crystal Growth, v. 55, p. 510–516.

Van Erk, W., 1982, Growth of a mixed crystal from an ideal dilute solution: Journal of Crystal Growth, v. 57, p. 71–83.

Voloshin, A. E., Glikin, A. E., Kovalev, S. I., and Rudneva, E. B., 2003a, Morphological effects in liquid phase epitaxy (the $C_8H_5O_4K$-$C_8H_5O_4Rb$-H_2O system): Crystallography Reports, v. 48, p. 1064–1075.

Voloshin, A. E., Kovalev, S. I., Rudneva, E. B., and Glikin, A. E., 2003b, Phenomena and mechanisms of mixed crystal formation in solutions II. Mechanisms of interface processes: Journal of Crystal Growth, v. 261, p. 105–117.

Voronkov, V. V., and Chernov, A. A., 1967, Entrapment of an impurity during the movement of an elementary step: Soviet Physics Crystallography, v. 12, p. 186–191.

Wasylenki, L. E., Dove, P. M., Wilson, D. S., and De Yoreo, J. J., 2005, Nanoscale effects of strontium on calcite growth: An *in situ* AFM study in the absence of vital effects: Geochimica et Cosmochimica Acta, v. 69, p. 3017–3027.

Zhmurova, Z. I., and Khaimov-Mal'kov, V. Ya., 1970a, Relation of impurity distribution to growth rate in the crystallization of isomorphous systems from solution: Soviet Physics Crystallography, v. 15, p. 108–111.

——— 1970b, Distribution of isomorphous components in crystallization from aqueous solution: Soviet Physics Crystallography, v. 15, p. 112–115.